Autotrophic nitrogen polishing of secondary effluents : alkaline pH and residual nitrate control S0-driven denitratation for downstream anammox treatment

Autotrophic nitrogen polishing of secondary effluents: alkaline pH and residual nitrate control in obtaining S^0-driven denitratation for downstream anammox treatment

Yankai Xie[1], Michiel Van Tendeloo[1], Weiqiang Zhu[1], Lai Peng[1, 2], Siegfried E. Vlaeminck[1, *]

[1.] Research Group of Sustainable Energy, Air and Water Technology, Department of Bioscience Engineering, University of Antwerp, 2020 Antwerpen, Belgium

[2.] Hubei Key Laboratory of Mineral Resources Processing and Environment, Wuhan University of Technology, Wuhan, Hubei 430070, China

*Corresponding author.

E-mail: Siegfried.Vlaeminck@UAntwerpen.be

Abstract

Energy-lean nitrogen removal, such as partial nitritation/anammox, often encounters effluent issues by accumulated nitrate and residual ammonium. This study proposed a novel autotrophic polishing strategy by coupling sulfur-driven denitratation with anammox. To explore the opportunities in obtaining stable and sufficient nitrite accumulation, the effects of pH alternation, residual nitrate level, and biomass-specific nitrate loading rate (BSNLR) were investigated in an S^0-packed bed reactor at low hydraulic retention time (i.e., 0.2 h). Implementing pH and residual nitrite control strategies would be easier than BSNLR control in the practical polishment of secondary effluent. The alkaline pH could realize successful nitrite accumulation under 0 residual nitrate, and further intensify the accumulation under the increased residual nitrate level. The residual nitrate level was found to be positively correlated with the nitrite accumulation efficiency. At pH 8.5 and residual nitrate of 1.0±0.8 mg N L^{-1}, sulfur-driven denitratation could successfully maintain nitrite accumulation of 6.4±1.0 mg

NO_2^--N L^{-1}, ideally for the downstream anammox containing residual ammonium of around 5 mg N L^{-1}. Since *Thiobacillus* members play a key role in managing nitrite accumulation, their abundance should be guaranteed in the practical application.

Keywords: sulfurotrophic denitratation; low nitrate strength; nitrite reductases; biomass nursing; biofilm reactor;

1. Introduction

Partial nitritation/anammox (PN/A) is considered a resource- and cost-effective technology for autotrophic nitrogen removal from organic carbon-lean wastewater [1]. However, mainstream PN/A processes, operated on sewage, have frequently met effluent issues by excessive accumulation of nitrate (NO_3^-) above 10 mg N L^{-1} [2-5]. Besides, some residual ammonium (e.g., around 5mg N L^{-1}) is required in mainstream PN/A systems to provide kinetic superiority for aerobic and anoxic ammonium-oxidizing bacteria over nitrite-oxidizing bacteria (NOB) [6]. Therefore, to satisfy the increasingly stringent discharge limitation of total nitrogen concentrations in the world (e.g., from 10-15 mg L^{-1} to 6 mg L^{-1} in the European Union) [7, 8], an additional polishing step is essential to remove both ammonium and nitrate in mainstream PN/A effluent.

Recently, an innovative denitratation/anammox technology has been proposed, where the nitrite (NO_2^-) anoxically reduced from nitrate would be removed together with NH_4^+ via the anammox process. Sufficient and stable nitrite accumulation via the denitratation process is the crucial prerequisite for a desirable polishing performance, as the anammox process could be readily steered as long as nitrite is available [9-11]. Various carbon sources such as acetate, ethanol, and methanol were studied to realize heterotrophic denitratation [9, 12, 13]. In addition, reduced sulfur compounds (e.g., sulfide and thiosulfate) were demonstrated to be alternative electron donors for

denitratation processes [14]. However, those carbon resources were more costly than those sulfur-based electron donors. For example, the NO_2^--N production by using sodium acetate as an electron donor was approximately 1.1 € kg^{-1}, while that of sodium thiosulphate pentahydrate was 0.83 € kg^{-1} (Table S3). Moreover, the sludge yields of heterotrophic denitratation (0.4-0.9 g cell g^{-1} nitrate) are higher than that of autotrophic denitratation (0.4-0.5 g cell g^{-1} nitrate) [15, 16]. Thus, autotrophic denitratation should be advocated as a more promising alternative.

Compared to the well-investigated sodium thiosulfate and the dangerous sodium sulfide, elemental sulfur (S^0) could be another appealing electron-donor candidate for autotrophic denitratation. Sulfur particles are more readily available, handleable, and inexpensive (i.e., around 0.06 € kg^{-1} NO_2^--N production, Table S3), and can even serve as biofilm carriers of packed bed reactors [14, 17]. There are several significant advantages of attached growth against suspended systems, such as automatic liquid and solid separation, ease of biomass growth, longer sludge retention time (SRT), high feasibility of short hydraulic retention time (HRT) control, and robustness against external stress [1]. Although a few studies have combined S^0-driven denitratation with the Anammox process in a single reactor [18, 19], the feasibility of S^0-packed-bed denitratation in polishing low N strength secondary effluent has not been reported. Moreover, the specific denitratation performance, influence factors, and mechanisms of the sulfur-driven denitratation are still not clear.

The bulk pH has a strong impact on both the heterotrophic and autotrophic denitrification processes, and the alkaline pH of 7.8-9.2 could benefit the nitrite accumulation (i.e., denitratation) [20-24]. This was probably related to the reductase activities, as the activity of nitrate reductases could outcompete that of nitrite reductases for electrons at alkaline conditions. Medium to high-strength nitrate medium (e.g., 100-2200 mg NO_3^--N L^{-1}) has been tested to realize denitratation [21, 24, 25]. However, the

77 denitratation feasibility of low-strength secondary effluent has not yet been reported.
78 Based on the balance between the effects of alkaline pH on denitratation and the cost
79 in maintaining the bulk alkalinity, medium alkaline pH (e.g., pH 8.5) would probably
80 be more promising in practical application. Moreover, since neutral pH (e.g., pH 7.0)
81 was generally applied in mainstream PN/A [2, 26, 27], it could be set as a baseline to
82 better understand the performance of medium alkaline pH on the denitratation of low-
83 strength secondary effluent.

84 According to a substrate counter-diffusion model, the soluble sulfur species
85 diffuse from the S^0 surface into the attached biofilm, while nitrate diffuses from the
86 bulk liquid into the biofilm [28]. Thus, when nitrate is reduced in the S^0-based biofilm,
87 nitrite may accumulate and diffuse into the bulk liquid. In the S^0-driven denitrification
88 process, the maximum specific substrate utilization rate of nitrate is around 1.8 times
89 higher than that of nitrite [29]. In other words, the residual nitrate levels could affect
90 the extent of nitrite accumulation [28-31]. The inherent features of sewage (e.g.,
91 fluctuant nitrogen strength and loading rates) and the dynamic changes of NOB activity
92 in the mainstream PN/A process could result in the fluctuation of nitrate level in the
93 secondary effluents [2, 32, 33]. Thus, the nitrate level in the influent of S^0-packed bed
94 reactors would fluctuate, which may further affect the residual nitrate and even the
95 accumulated nitrite levels. Since the nitrate reductases have a greater affinity for
96 reduced electron carriers than that of nitrite reductases [34], the diffusion extent of
97 nitrate and reduced electron carriers in biofilm may influence nitrite dynamics.
98 However, it is rarely feasible to maintain the desired biofilm thickness due to its growth,
99 detachment, and predation over time [29]. The specific NO_3^--N loading rate based on
100 biomass could be a more accessible alternative to manipulate the substrate counter-
101 diffusion, consequently to the nitrite accumulation. Therefore, it is possible to realize
102 sulfur-driven denitratation by controlling the residual nitrate level and biomass-specific

nitrate loading rate (BSNLR).

Considering that previous studies focused on the medium- to high-strength denitratation in long HRT (e.g., 0.5-24 h) (Table S1), it is necessary to fill in the gaps of low-strength denitratation in short HRT (e.g., ≤ 0.2 h) that could be coupled to the downstream anammox process for autotrophically polishing the secondary effluents in reality. To the best of our knowledge, there is hardly any study looking into the feasibility of S^0-driven denitratation for stable and sufficient nitrite accumulation in the polishing process of secondary effluent (e.g., 15 mg NO_3^--N L^{-1}). In this study, three control parameters, i.e., the bulk pH, residual nitrate level, and BSNLR were implemented to investigate the long-term feasibility (max. 130 days) of a successful sulfur-driven denitratation process in an S^0-packed bed reactor. Unlike most previous denitratation studies (Table S1), the reactor temperature here was controlled relatively low (i.e., 21±1 °C) to further broaden its applicability in practice. The correlation analysis of the control parameters (residual nitrate level and BSNLR) and nitrite accumulation efficiency (NAE) was implemented. Additionally, the evolution of microbial community composition in the biofilm was analyzed to investigate the key microbial species that play a key role in realizing the ideal sulfur-driven denitratation process.

2. Materials and methods

2.1 Reactor setup

An S^0-packed bed reactor was set up independently in this study, with a total volume of 1 L (inner diameter 7.4 cm and height 23.3 cm) and a bed volume of 0.8 L (including void volume). Pure S^0 particles of 3-4 mm diameter were used as both electron donors and biofilm carriers. The reactor was operated in up-flow mode. During the long-term operation, two continuous influent flowrates (43 and 86 L d^{-1}) were

employed by a peristaltic pump (Seko Peristaltic Pumps, PR7), and the influent flow rate of 86 L d^{-1} was only imposed for short periods (days 109-124) to raise the nitrate loading rate (NLR). Based on the S^0 void volume and free reactor volume (tubing volume and upper space of S°bed), two HRT settings (i.e., 0.1 and 0.2 h) were involved. In addition, a recirculation rate of 1382 L d^{-1} was imposed to give entirely mixed conditions, via a peristaltic pump (Etatron BH3-V Peristaltic Pump) [15, 28].

2.2 Chemicals and influent

The low-strength synthetic influent contained 5.6±0.7 mg NH_4^+-N L^{-1} and 12.9±0.6 mg NO_3^--N L^{-1} to mimic the poor-quality secondary effluent of mainstream PN/A processes. It should be noted that the nitrate concentration once increased to 17.7±0.1 mg NO_3^--N L^{-1} (days 81-88) and 22.4±1.0 mg NO_3^--N L^{-1} (days 89-94), which were in the normal range of some mainstream PN/A effluent [2, 35]. Sodium bicarbonate (130 mg HCO_3^- L^{-1}), sodium dihydrogen phosphate (1 mg P L^{-1}), and 0.1 mL L^{-1} of trace element solutions A and B were added into influent to mimic the alkalinity of general effluent and avoid the limitation of microbial growth [36, 37]. To simulate the realism of the anoxic effluent, especially of two-stage PN/A systems [1], the influent tank was sealed, and the influent was maintained anoxic by regularly sparging with nitrogen gas (N_2).

2.3 Reactor operation

The reactor was inoculated with 1 g VSS L^{-1} activated sludge from a municipal wastewater treatment plant (WWTP, Aquafin Antwerpen-Zuid, Belgium) to enrich sulfur-oxidizing bacteria [38, 39]. It was operated in a temperature-controlled room at 21±1 °C and continuously fed with anoxic influent. Thus, the reactor could maintain an anoxic condition and suppress ammonium consumption via aerobic ammonium-oxidizing bacteria.

153 The reactor pH was controlled at neutral (7.1±0.1) or alkaline (8.5±0.1) conditions
154 by indirectly dosing sodium hydroxide into the influent. The pH in the reactor was
155 periodically monitored with a Hanna Edge pH meter (HI2002-02) equipped with a
156 Hanna pH electrode (HI-12301). The whole operation period (130 days) was divided
157 into seven phases based on different pH setpoints in the reactor, which were highlighted
158 in Fig.2. The alteration of pH setting points between each phase aimed to benefit the
159 investigation of pH 8.5 on the S^0-driven denitratation process. The HRT of 0.1 h was
160 implemented during days 109-124 of phase VII, while that of 0.2 h was used in all the
161 other periods. The residual nitrate level in the reactor was controlled by adjusting the
162 influent nitrate concentrations (12.9-22.4 mg NO_3^--N L^{-1}, phase VI), and flowrates of
163 influent (43 and 86 L d^{-1}, phase VII) as mentioned in section 2.2 and 2.1, respectively.
164 Since the BSNLR was determined by the volumetric NLR and biomass concentration
165 in the reactor, controlling the residual nitrate level would inevitably affect the BSNLR.
166 In the S^0-packed bed reactor, no suspended biomass (i.e., flocs) was observed in the
167 effluent, so the biomass level monitoring and control were implemented every week,
168 by taking 5 ml out of the total 800-ml well-mixed S^0 particles and using anoxic water
169 to wash off the biofilm attached to S^0 particles. The sampled biomass was preserved at
170 4 °C for further concentration and community analysis.

171 **2.4 Analytical and calculation methods**

172 To monitor the reactor performance, influent and effluent samples were collected
173 periodically from the outlets of the influent and effluent pumps, respectively. These
174 samples were immediately filtered using 0.2 μm filters (CHROMAFIL Xtra PVDF),
175 and stored at 4 °C until analysis. NH_4^+-N, NO_2^--N, and NO_3^--N were measured with
176 the San++ Automated Wet Chemistry Analyzer [2, 40]. The biomass level in the reactor
177 was measured in triplicate based on volatile suspended solids (VSS) using standard
178 methods [41] and calculated based on the S^0-bed volume of 0.8 L.

The calculations used to determine the nitrate removal efficiency (NRE), NAE, NLR, BSNLR, and biomass-specific nitrite accumulation rate (BSNAR) were shown in eq. (1)-(5). NRE was calculated based on the influent NO_3^--N concentration ($In_{NO_3^-N}$) and effluent NO_3^--N concentration ($Ef_{NO_3^-N}$). NAE refers to the ratio of the produced NO_2^--N ($P_{NO_2^-N}$) and the reduced NO_3^--N concentration. The NLR calculation was based on $In_{NO_3^-N}$, influent flow rate (Q_{in}), and S^0-bed volume (V_{s^0}). BSNLR refers to the ratio of NLR and biomass concentration (C_{BM}) in the reactor. The BSNAR calculation was based on $P_{NO_2^-N}$, influent flow rate (Q_{in}), S^0-bed volume (V_{s^0}), and C_{BM}. For all the measured and calculated data in relevant operating phases, Spearman's correlation was analyzed (IBM® SPSS® Statistics 26) to explore the correlation of control parameters (BSNLR and residual nitrate level) with NAE. Statistical significance was defined as a p-value of less than 0.05 [42].

$$NRE = \frac{In_{NO_3^--N} - Ef_{NO_3^--N}}{In_{NO_3^--N}} \times 100\% \quad (1)$$

$$NAE = \frac{P_{NO_2^--N}}{In_{NO_3^--N} - Ef_{NO_3^--N}} \times 100\% \quad (2)$$

$$NLR = \frac{In_{NO_3^--N} \times Q_{in}}{V_{S0}} \quad (3)$$

$$BSNLR = \frac{In_{NO_3^--N} \times Q_{in}}{V_{S0} \times C_{BM}} \quad (4)$$

$$BSNAR = \frac{P_{NO_2^--N} \times Q_{in}}{V_{S0} \times C_{BM}} \quad (5)$$

2.5 Microbial community analysis

To analyze the evolution of microbial community composition, biomass samples were collected from the S^0 reactor for microbiome analysis during the operation period. Samples were stored at −20 °C before DNA extraction. According to the manufacturer's instructions, DNA was extracted using a PowerFecal® DNA isolation kit (QIAGEN, Germany). The DNA extracts were sent to Novogene (UK) Co., Ltd for

microbial community analysis like our previous studies [43]. 16S rRNA genes of 16S V3 were amplified using specific primers 338F (5'- ACT CCT ACG GGA GGC AGC AG -3') and 518R (5'- ATT ACC GCG GCT GCT GG -3'). Moreover, the alpha diversity (Shannon's) and beta diversity (Bray-Curtis dissimilarity) were analyzed in every sample and between different samples to characterize the variation in the microbial community, respectively.

3. Results and discussion

The sulfur-driven denitratation of the synthetic secondary effluent was carried out in an S^0-packed bed reactor. Due to the anoxic condition in the reactor, the NH_4^+-N loss was negligible, with a ratio of 2±2%, and the NH_4^+-N concentration in the effluent was at 5.2±0.4 mg L^{-1} (Fig. 1). The anoxic conditions successfully inhibited the activity of ammonium-oxidizing bacteria (AOB) in the sulfur reactor. As shown in Fig. 2b, the NAE is always below 100%, indicating that the sulfur-driven denitrification (i.e., NO_3^--N to N_2) existed during the whole experiment. Since no carbon sources were added to the prepared influent, heterotrophic denitratation was suggested to be negligible in this S^0-based reactor [24, 38]. To achieve the stoichiometric ratio of 1.3 NO_2^-/1 NH_4^+ for the downstream anammox treatment, stable nitrite accumulation at approximately 6.5 mg N L^{-1} is necessary for the bulk ammonium of around 5 mg N L^{-1} [1].

3.1 Effects of pH control

The pH control strategy was implemented over the whole operation period. In the start-up stage (phase I), the reactor pH was controlled at around 7.1±0.1 as a baseline. The effluent nitrate stabilized at around 0 within 10 days and no nitrite was detected, indicating the S^0-based reaction approached the complete denitrification (Fig. 2a). Then the reactor pH was increased to alkaline pH condition (i.e., 8.5±0.1) to evaluate its effect on nitrite accumulation performance.

After switching to pH 8.5, both nitrite accumulation and residual nitrate appeared immediately. The pH shock observably disturbed the denitratation and denitritation (e.g., from NO_2^--N to N_2) processes, with NRE decreasing from 96±2% to 26% but NAE increasing from 0 to 48% on day 10 (Fig. 2b). With the recovery of nitrate removal, the nitrite concentration gradually increased to 6.8 mg N L^{-1} at day 16 (Fig. 2a). Combining with the effluent NH_4^+-N level, the accumulated NO_2^--N could reach the ideal anammox ratio (i.e., 1.3 NO_2^-/1 NH_4^+, Fig. 3) [1]. However, the nitrite accumulation declined in the later phase II. Surprisingly, after changing the pH back to neutral, the nitrite accumulation level and efficiency immediately turned into a growing trend, which was different from its no accumulation performance in phase I (pH 7). In phase IV, switching back to pH 8.5 made the nitrite accumulation performance thrive again. Successful S^0-driven denitratation was achieved with stable nitrite accumulation concentration and rate at 6.4±1.0 mg N L^{-1} and 353±51 mg N L^{-1} d^{-1}, respectively (Fig. 2). When switching to pH 7.1±0.1in phase V, the previously ideal nitrite level unexpectedly declined. The contradictory nitrite accumulation performance of phase III and phase V is probably attributed to the different levels of residual NO_3^--N, which were 1.6±0.4 mg N L^{-1} and 0.4±0.2 mg N L^{-1}, respectively. Based on the successful alkaline-pH-promotion of denitratation in phase II and phase IV, the decreasing trend of nitrite accumulation in phase V was reversed in phase VI by switching to pH 8.5.

From phase I to phase VI, switching pH from neutral to alkaline level could always promote nitrite accumulation. The dynamic changes of the denitratation and denitritation processes are closely related to the nitrate and nitrite reductases, respectively [44, 45]. It was proposed that nitrite could accumulate at high pH because the activity of nitrate reductases could outcompete that of nitrite reductases for electrons, and the nitrite reductases were more sensitive to alkaline environments than nitrate reductases [24, 46]. Previous studies about facultative autotrophic denitrifiers

suggested that the protons (H^+) required for nitrate reduction come from the inside of cytoplasmic membrane, whereas nitrite reductases receive the protons from the outside [47, 48]. At pH 8.5, protons could be relatively scarce outside the cytoplasmic membrane, inhibiting nitrite reduction [20, 49]. The nitrite reductases could not readily adapt to the pH 8.5-shock. In contrast, based on the nitrate removal performance from phase I to phase VI, the nitrate reductases adapted to the pH 8.5-shock in 4 days (phase II). Subsequently, the NRE sustained almost untouched in phase III-VI (Fig. 2b), suggesting that the nitrate reductases could easily adapt to pH shock. Compared to the up and down of NAE (0-72%) in phase II, the relatively stable NAE (54±9%) in phase IV means that the stimulation efficacy of pH 8.5-shock on nitrite accumulation became long-acting, namely, the capacity of denitrifiers in adjusting the adaptation speed of nitrite reductases presumably weakened.

It was suggested that alkaline conditions (i.e., pH 7.8-9.2) could facilitate the denitratation process [20-24]. Chen et al. (2018) investigated the effects of different pH setpoints (i.e., 6.0, 6.5, 7.0, 7.5, 8.0, 8.5, and 9.0) on nitrite accumulation in the sulfur denitrification process, and found that bulk pH of 8.5 could realize the highest NAE [24]. Huo et al. (2022) dosed siderite to stabilize the pH of an anammox-coupled sulfur-driven denitrification (ASD) reactor at around 8.5, achieving efficient nitrogen removal from leachate [18]. Since the secondary effluents after the mainstream PN/A treatment were generally close to near-neutral pH [2, 26, 27], additional alkalis would be required to sustain the alkaline environment for the subsequent denitratation process. Given the expenditure of alkali dosage, medium alkaline pH of 8.5±0.1 was adopted in the S^0-packed bed reactor, which was consistent with the suggested optimum pH for autotrophic denitratation. As a result, the long-acting denitratation of low-nitrate-strength wastewater was realized under this alkaline pH in a short HRT of 0.2h.

3.2 Effects of residual nitrate level

The residual nitrate concentration in the S^0-packed bed reactor was controlled by separately adjusting the NLR, involving the influent nitrate concentrations (12.9-22.4 mg NO_3^--N L^{-1} in phase VI) and flowrates (43 and 86 L d^{-1} in phase VII).

In phase VI, the influent nitrate concentration stepwise increased from 12.3±0.2 mg N L^{-1} to 17.7±0.1 mg N L^{-1} and 22.4±1.0 mg N L^{-1}, then decreased back to 12.3±0.2 mg N L^{-1}. Accordingly, the effluent nitrate concentration stepwise increased from 1.1±0.5 mg N L^{-1} to 3.3±2.2 mg N L^{-1} and 5.2±0.9 mg N L^{-1}, then decreased back to 1.0±0.9 mg N L^{-1} (Fig. 2a). After switching the neutral pH in phase V to alkaline pH in phase VI, the effluent nitrite level gradually increased from 2.0±0.7 mg N L^{-1} to 5.1±0.6 mg N L^{-1} at the residual nitrate of 1.1±0.5 mg N L^{-1} (day 71-day 82). With the gradual increase of residual nitrate concentration, the nitrite accumulation further increased to 10.8±1.3 mg N L^{-1} (day 83-day 88) and 13.2±1.2 mg N L^{-1} (day 89-day 94). Interestingly, once the residual nitrate level decreased to 1.0±0.9 mg N L^{-1} (days 95-105), the nitrite level fell to 4.3±0.7 mg N L^{-1}. Thus, increasing the residual nitrate concentration benefited the nitrite accumulation, which was consistent with the previous sulfur-driven denitrification studies [29, 31]. In phase VII, instead of raising the influent nitrate concentration, the influent flow rate was doubled (day 108-day 124), increasing the residual nitrate concentration from 1.6±0.2 mg N L^{-1} to 4.9±0.6 mg N L^{-1}. The increased residual nitrate level contributed to the promotion of nitrite accumulation from 3.2±0.4 mg N L^{-1} to 4.9±0.8 mg N L^{-1}.

In this study, controlling the residual nitrate level was regarded as a strategy in obtaining S^0-driven denitratation for secondary effluent polishment, while the residual nitrate level itself was an indicator or "result". To further understand the relationship between residual nitrate level and NAE, Spearman's correlation analysis was implemented for the entire and separate phases (Table 1a). The correlation coefficient

(ρ) of the whole experiment (phases I-VII) was moderately positive (ρ= 0.49, p< 0.0001). At the same pH condition of 8.5, the period lengths of phase IV and phase VI were relatively close, with 34 and 31 days, respectively. The fair correlation coefficient in phase IV (ρ= 0.39, p= 0.05) and the strong correlation coefficient in phase IV (ρ= 0.87, p= 0.02) further revealed that the residual nitrate level and NAE were positively correlated.

In the sulfur compound (e.g., S^{2-} and $S_2O_3^{2-}$)-driven denitratation process, the S/ NO_3^--N ratio was an important factor affecting the performance of nitrite accumulation [25, 50, 51]. When the sulfur beads were used as electron donors, the reaction-dose control depended on the activity of sulfurotrophs and the counter-diffusion rate. In this case, only the available sulfur (i.e., the solubilized sulfur) can be taken into account, which is not facile to control, especially in an S^0-packed bed reactor [28, 52, 53]. Therefore, controlling the S/NO_3^--N ratio via adjusting the residual nitrate level was more flexible in practical operation. Based on the declined performance of nitrite accumulation in phase V, switching the alkaline pH (phase VI) to neutral pH (phase VII) should have caused the collapse of nitrite accumulation, whereas the stable and high nitrite level was actually obtained, attributed to the effect of high residual nitrate concentration. Although the residual nitrate level of phase VI (day 89-day 94) and phase VII (day 108-day 124) were similar (i.e., around 5 mg N L^{-1}), the effluent nitrite concentration of the former was over two times of the latter, indicating the nitrite accumulation potential could be further reinforced by alkaline pH. When zooming into phase IV, it is remarkable to find that the performance of nitrite accumulation was not always affected by the residual nitrate level. This seeming paradox is exactly the reason why the positive correlation in Phase IV was weaker than that in Phase VI. During day 48-day 55 (phase IV), the ideal nitrite level of 6.7±0.2 mg N L^{-1} under 0 residual nitrate further demonstrated the capability of alkaline pH 8.5 on the stimulation of the

denitratation process.

3.3 Effects of BSNLR control

The dynamic changes of BSNLR were controlled based on the volumetric NLR and biomass concentration in the reactor. The biomass concentration in the S^0-packed bed reactor was monitored and controlled during the whole experiment and maintained in a range of 2.3-6.2 g VSS L^{-1} (Fig. S1). The successful nitrite accumulation (i.e., 6.4±1.0 mg N L^{-1}) for anammox was obtained at BSNLR of 150±42 mg N g^{-1} VSS d^{-1} in phase IV. To understand the association between BSNLR and the corresponding NAE more explicitly, Spearman's correlation analysis was implemented (Table 1b). There was a strong positive correlation between the BSNLR and NAE (ρ= 0.6, $p<$ 0.0001). Besides, there was also a very strong positive correlation between the BSNLR and BSNAR (ρ= 0.78, $p<$ 0.0001). The positive correlation indicated that increasing the BSNLR could potentially benefit the nitrite accumulation performance.

However, under the neutral pH conditions, the BSNLR of phase VII (491±25 mg N g^{-1} VSS d^{-1}) was roughly two times higher than that of phase III (244±8 mg N g^{-1} VSS d^{-1}), whereas they obtained similar levels of nitrite accumulation and NAE (Fig. 2). Since S^0 is poorly soluble in water, sulfur-oxidizing bacteria (SOB) producing extracellular enzymes can convert S^0 into soluble polysulfides (S_n^{2-}), which then diffuse into the biofilm as electron donors [29, 54]. As shown in Fig. 2a, the residual nitrate level of phase VII (4.9±0.6 mg N L^{-1}) was much higher than that of phase III (1.5±0.4 mg N L^{-1}), hence the nitrite accumulation performance of phase VII was more likely due to the decreased S/NO_3^--N ratio in the attached biofilm [25, 50, 51]. Moreover, based on the same biomass levels (3.0±0.2 g VSS L^{-1}) in phase III and phase VII, it was suggested that the relative abundance of sulfurotrophic communities related to S^0-driven denitratation became insufficient in phase VII.

According to the counter-diffusion theory, raising BSNLR means the intensification of nitrate penetration into the attached biofilm via increasing the nitrate loading and/or decreasing the biomass concentration [28]. It is noted that there was a high positive correlation between BSNLR and residual nitrate level ($\rho = 0.73$, $p < 0.0001$) (Table 1b). Actually, the presence of residual nitrate is not only a control strategy but also an indicator of nitrite accumulation. Since the nitrate and nitrite reduction reactions occur in series, if the consumption reaction of nitrate is faster than that of nitrite, the presence of nitrate could imply the accumulation of nitrite. All the analyzed parameters (i.e., pH, residual nitrate, and BSNLR) are related to the kinetics of these processes. In each period of operation, the system will have a certain capacity to reduce nitrate and nitrite, which will depend on both the pH value, the biomass concentration, and its abundance of sulfurotrophic communities. On the other hand, the nitrogen load applied varied in some periods of operation (e.g., phase VII). Thus, nitrite buildup would occur when the applied nitrogen load exceeded the denitritation capacity of the reactor. Considering the complexity of BSNLR control via managing the biomass level and the abundance uncertainty of denitrifying bacteria, the pH control and the residual nitrate control were more facile and explicit to obtain S^0-driven denitratation in such packed-bed-biofilm reactors.

3.4 Evolution of the microbial community in the long term

The microbiome analysis in the S^0-packed bed reactor was implemented to evaluate their contribution to sulfur-driven denitratation during the long-term operation. Based on the Bray-Curtis dissimilarity analysis, the variation in the microbial community between the first sample and each subsequent sample became more significant over time, indicating the community shift during the experiment (Fig. 4 and Fig. S2). The Shannon index showed a decreasing trend from 1.8 to 0.9, meaning richness and diversity reduced over the long-term operation. Among all the putative

sulfurotrophs shown in Fig. 4, *Thiobacillus*, *Sulfurimonas*, and *Chlorobi_bacterium_OLB5* were the three most abundant genera. *Thiobacillus* and *Sulfurimonas* belong to the sulfur autotrophic denitrification bacteria that could use elemental sulfur as electron donors to reduce nitrate or nitrite [55]. *Chlorobi_bacterium_OLB5* could be a type of green sulfur bacteria that uses sulfur and carbon dioxide (CO_2) as the electron donor and acceptor respectively to produce organic matter [56]. Compared to the day-24 sample (phase I), the day-30 sample showed a visible increase in the abundance of *Thiobacillus* (from 11.8% to 14.4%), indicating their enrichment at pH 7.1±0.1. From day 30 to day 126, the relative abundance of *Thiobacillus* decreased stepwise from 14.4% to 0.8% (Fig. 4), probably ascribed to the adverse effect of pH 8.5 on their proliferation. In other words, the pH alternation between 7.1 and 8.5 resulted in the inevitable change of microbial community structure over the whole experimental period.

From the angle of nitrite accumulation, the NAE became more stable and enduring (54±9% over 30 days) in phase IV compared to that of phase II, indicating the sulfurotrophs got weaker in adjusting the adaptation speed of nitrite reductases to pH 8.5-shock. The self-adjusting capacity of microbes could be positively correlated to their relative abundance [57]. Since the relative abundance of *Thiobacilus* showed a decreasing trend after phase III, it could be a key species in obtaining successful denitratation. As shown in phase VII of Fig. 2c, the roughly two-fold BSNLR of phase III could not contribute the same fold of nitrate accumulation rate. This could be related to the relative abundance of *Thiobacillus*, which in phase VII (0.8%, day 126) was less than 6% of that in phase III (14.4%, day 30). Hence, the higher BSNLR in phase VII means that the NLR was beyond the capability of *Thiobacillus* to accumulate more nitrite. By the way, the high residual nitrate level indicates the capacity of denitrifiers was insufficient under the high NLR in phase VII.

According to Spearman's correlation analysis between the relative abundance of *Thiobacillus* and nitrite accumulation performance, there was a very high positive correlation between its relative abundance and NAE (ρ= 0.9, p= 0.004, Table S2). Thus, the genus *Thiobacillus* was the critical community to control nitrite accumulation. Bulk pH is considered a decisive factor in bacteria survival. The optimum growth pH of *Thiobacillus* was demonstrated to be 6.8-7.4 [55], thus the long-term operation out of their optimum pH range probably caused the shrinkage of their relative abundance. Additionally, *Sulfurimonas* is one of the most commonly reported sulfur-based autotrophic denitrifying genera as well [38, 55, 58]. They competed with *Thiobacillus* for substrate and became the dominant genera in phase VII. To our knowledge, this is the first time that the long-term effect of pH on microbial community shift in sulfur-driven denitratation has been reported.

3.5 Application potential

The S^0-driven denitratation under the low-nitrate-strength wastewater of around 13 mg N L^{-1} was investigated in the packed-bed biofilm reactor for the first time, which realized 54±9% of NAE under the NLR of 0.71g N L^{-1} d^{-1}. There are several studies on nitrite accumulation via heterotrophic or autotrophic denitratation for medium-strength nitrate-containing wastewater (e.g., 50-101 mg N L^{-1}) under the NLR of 0.1-2.4 g N L^{-1} d^{-1} (Table S1) [9, 24, 25, 51, 59]. Besides, high-strength nitrate denitratation (i.e., 364-2200 mg N L^{-1}) was also reported in previous studies when using organic carbon sources as electron donors [21, 60]. Although the heterotrophic denitratation process could obtain a relatively high NCE of 75-97% (Table S1), the higher sludge production rate would further increase the operating expense via sludge disposal, which could be more suitable for treating the high chemical oxygen demand wastewater. Compared to sulfide or thiosulfate for autotrophic denitratation, elemental sulfur is less expensive and more user-friendly in practice. With the biofilm grown on carrier materials (i.e., S^0

particles), flocs were neither observed either in the packed-bed reactor nor in its effluent. In practice, the flocs containing AOB and NOB that came from the mainstream PN/A system would not affect system performance, mainly due to the anoxic condition in the S^0-packed bed reactor [61]. During the whole experiment, the anoxic environment enabled sulfur-driven denitrification as the amount of the produced nitrite could not match that of the removed nitrate (i.e., NAE<100%). Thus, the denitrification efficiency was negatively related to the NAE. Nevertheless, in whole phase IV, the produced NO_2^--N (around 6.5 mg N L^{-1}) together with the intrinsic NH_4^+-N (around 5 mg N L^{-1}) could satisfy the metabolism of anammox bacteria, converting around 10 mg N L^{-1} to N_2 gas and 1.3 mg N L^{-1} as nitrate [1, 62]. Combined with the residual nitrate of 1.0±0.8 mg NO_3^--N L^{-1}, there would be only 2.3±0.8 mg NO_3^--N L^{-1} [1] as total inorganic nitrogen left in the final effluent.

As aforementioned, the implementation of pH and residual nitrite control strategies would be easier than the BSNLR control in the practical polishment of secondary effluent. Although the nitrate strength is quite low and even fluctuates in real-world scenarios, successful nitrite accumulation could win the opportunity for downstream anammox polishment. The individual alkaline pH control with low/no residual nitrate level could be sufficient for relatively low nitrate and ammonium strength scenarios (e.g., phase IV), while combining the alkaline pH and relatively high residual nitrate level (by increasing NLR) could produce more nitrite, which is suitable for high nitrate and ammonium strength scenarios.

Although the alkaline pH control could effectively stimulate and maintain the S^0-driven denitratation process, it has the potential to reduce the relative abundance of *Thiobacillus*, which could be a critical community in realizing nitrite accumulation. It can be predicted that its relative abundance would further decrease to 0 under the alkaline condition. Due to the beneficial effects of neutral pH on *Thiobacillus*

enrichment, *Thiobacillus* could be nursed at pH 7 and stored at 4 °C under nitrate preservation [1]. In the full-scale application, updating the reactor with the stored biomass is a possible backup when the efficacy of the alkaline control gets weaker. Considering the long-term operation of the system, the replenishment of sulfur particles would be inevitable. In the design of a full-scale packed-bed reactor, a certain number of side openings along the reactor height would benefit the biomass updation and/or sulfur replenishment. To further reduce the occupied area and the costs of basic construction and operation, the integration of S^0-driven denitratation and anammox processes in a single-stage packed-bed reactor can be expected in the future study. The anoxic and alkaline environment together with the S^0 carriers could support the growth of anammox bacteria [2, 63, 64]. Besides, to avoid microbial adaptation to the persistent alkaline pH environment, directly switching the neutral pH could be a possible strategy when the influent nitrate loading is relatively high like that in phase VII. However, the frequency and duration of pH alternation may depend on the practical situation and require further investigation.

The autotrophic denitratation/anammox process could be more energy-saving than the nitrification/denitrification process in nitrogen removal from the wastewater containing both ammonium and nitrate, because the latter process requires extra aeration to complete nitrification. Since the mainstream PN/A process itself is considered an energy-neutral or energy-positive wastewater treatment process, the proposed polishment strategy here could strengthen and even promote the application of mainstream PN/A. Moreover, it is tricky to precisely consume the dosed carbon resources in the heterotrophic denitratation process, probably causing secondary pollution of the organic substances in the effluent [38]. Previous studies suggested that sulfate was the sulfur species that would be released into the bulk environment during the S^0-driven denitratation process [14, 24]. Currently, there is no discharge limitation

485 of sulfate in the legislative regulation of the European Commission [7]. In contrast to
486 heterotrophic denitratation, the S^0-driven denitratation could avoid the release of
487 greenhouse gas (i.e., CO_2) into the environment, contributing to the reduction of the
488 overall environmental footprint and climate impact of wastewater treatment. Compared
489 to carbon sources added in the heterotrophic denitratation process, the element sulfur
490 used in autotrophic denitratation is much cheaper (Table S3). Therefore, the S^0-driven
491 denitratation in a packed-bed reactor has the potential to polish the secondary effluent
492 in wastewater treatment plants with low nitrate levels but high volumetric loading due
493 to its short HRT (i.e., 0.2 h).

494 **4. Conclusions**

495 The pH control and the residual nitrate control should be more facile and explicit
496 than the BSNLR control to obtain S^0-driven denitratation in the packed-bed reactor.
497 The alkaline pH of 8.5 could effectively stimulate and maintain nitrite accumulation
498 over the long-term operation. The residual nitrate level was controlled by adjusting the
499 influent nitrate loading rate and positively correlated to the NAE. The nitrite
500 accumulation performance could be reinforced by the combination of the alkaline pH
501 and residual nitrate control. Under pH 8.5 and residual nitrate of 1.0±0.8 mg N L^{-1},
502 stable and sufficient nitrite accumulation could be obtained for the downstream
503 anammox treatment at a short HRT of 0.2 h. The genus *Thiobacillus* played a crucial
504 role in S^0-driven denitratation and should be maintained in sufficient abundance.
505 Overall, it is possible to apply the S^0-driven denitratation/anammox process to polish
506 the secondary effluents in practice.

507 **Appendix A. Supplementary data**

508 E-supplementary data of this work can be found in the online version of the paper.

Acknowledgments

This work was supported by the China Scholarship Council (No. CSC201706130131). The authors would like to thank Dr. Wannes Van Beeck for his guidance and help in the microbial DNA extraction step.

References

[1] S. Vlaeminck, H. De Clippeleir, W. Verstraete, Microbial resource management of one-stage partial nitritation/anammox, Microbial Biotechnology, 5 (2012) 433-448.
[2] L. Peng, Y. Xie, W. Van Beeck, W. Zhu, M. Van Tendeloo, T. Tytgat, S. Lebeer, S.E. Vlaeminck, Return-Sludge Treatment with Endogenous Free Nitrous Acid Limits Nitrate Production and N2O Emission for Mainstream Partial Nitritation/Anammox, Environmental Science & Technology, 54 (2020) 5822-5831.
[3] M. Van Tendeloo, Y. Xie, W. Van Beeck, W. Zhu, S. Lebeer, S.E. Vlaeminck, Oxygen control and stressor treatments for complete and long-term suppression of nitrite-oxidizing bacteria in biofilm-based partial nitritation/anammox, Bioresource Technology, (2021) 125996.
[4] P. Wu, J. Chen, V.K. Garlapati, X. Zhang, F. Wani Victor Jenario, X. Li, W. Liu, C. Chen, T.M. Aminabhavi, X. Zhang, Novel insights into Anammox-based processes: A critical review, Chemical Engineering Journal, 444 (2022) 136534.
[5] T. Liu, Y. Lu, M. Zheng, S. Hu, Z. Yuan, J. Guo, Efficient nitrogen removal from mainstream wastewater through coupling Partial Nitritation, Anammox and Methane-dependent nitrite/nitrate reduction (PNAM), Water Research, 206 (2021) 117723.
[6] V. Poot, M. Hoekstra, M.A.A. Geleijnse, M.C.M. Van Loosdrecht, J. Pérez, Effects of the residual ammonium concentration on NOB repression during partial nitritation with granular sludge, Water Research, 106 (2016) 518-530.
[7] E. Commission, Annexes to the proposal for a directive of the European parliament and of the council concerning urban wastewater treatment (recast), 2022.
[8] E.P.A. EPA, Compendium of state and regional NPDES nutrient permitting approaches, 2022.
[9] R. Du, S. Cao, B. Li, M. Niu, S. Wang, Y. Peng, Performance and microbial community analysis of a novel DEAMOX based on partial-denitrification and anammox treating ammonia and nitrate wastewaters, Water research, 108 (2017) 46-56.
[10] M. Kumar, J.-G. Lin, Co-existence of anammox and denitrification for simultaneous nitrogen and carbon removal—strategies and issues, Journal of Hazardous Materials, 178 (2010) 1-9.
[11] Q.-Y. Hu, D. Kang, R. Wang, A.-Q. Ding, G. Abbas, M. Zhang, L. Qiu, H.-F. Lu, H.-J. Lu, P. Zheng, Characterization of oligotrophic AnAOB culture: morphological, physiological, and ecological features, Applied microbiology and biotechnology, 102 (2018) 995-1003.
[12] S. Ge, Y. Peng, S. Wang, C. Lu, X. Cao, Y. Zhu, Nitrite accumulation under constant temperature in anoxic denitrification process: The effects of carbon sources and COD/NO3-N, Bioresource technology, 114 (2012) 137-143.
[13] B. Cui, X. Liu, Q. Yang, J. Li, X. Zhou, Y. Peng, Achieving partial denitrification through control of biofilm structure during biofilm growth in denitrifying biofilter, Bioresource technology, 238 (2017) 223-231.
[14] Y.-F. Deng, F.-x. Zan, H. Huang, D. Wu, W.-t. Tang, G.-H. Chen, Coupling sulfur-based denitrification with anammox for effective and stable nitrogen removal: A review, Water Research, 224 (2022) 119051.
[15] Metcalf, I. Eddy, Wastewater engineering: Treatment, disposal and reuse, McGraw-Hill New York,, USA, 1991.
[16] S.-E. Oh, K.-S. Kim, H.-C. Choi, J. Cho, I. Kim, Kinetics and physiological characteristics of autotrophic dentrification by denitrifying sulfur bacteria, Water science and technology, 42 (2000) 59-68.

[17] Y. Wang, J.P. Pavissich, F. Sabba, C. Bott, R. Nerenberg, Elemental sulfur (S) as a supplemental electron donor for wastewater denitrification, Proceedings of the Water Environment Federation, 2011 (2011) 1590-1597.
[18] D. Huo, Y. Dang, D. Sun, D.E. Holmes, Efficient nitrogen removal from leachate by coupling Anammox and sulfur-siderite-driven denitrification, Science of The Total Environment, 829 (2022) 154683.
[19] X. Li, Y. Yuan, Y. Huang, Z. Bi, Simultaneous removal of ammonia and nitrate by coupled S0-driven autotrophic denitrification and Anammox process in fluorine-containing semiconductor wastewater, Science of The Total Environment, 661 (2019) 235-242.
[20] W. Qian, B. Ma, X. Li, Q. Zhang, Y. Peng, Long-term effect of pH on denitrification: High pH benefits achieving partial-denitrification, Bioresource Technology, 278 (2019) 444-449.
[21] W. Li, X.-Y. Shan, Z.-Y. Wang, X.-Y. Lin, C.-X. Li, C.-Y. Cai, G. Abbas, M. Zhang, L.-D. Shen, Z.-Q. Hu, H.-P. Zhao, P. Zheng, Effect of self-alkalization on nitrite accumulation in a high-rate denitrification system: Performance, microflora and enzymatic activities, Water Research, 88 (2016) 758-765.
[22] R. Du, S. Cao, H. Zhang, X. Li, Y. Peng, Flexible Nitrite Supply Alternative for Mainstream Anammox: Advances in Enhancing Process Stability, Environmental Science & Technology, 54 (2020) 6353-6364.
[23] X. Zhang, Y. Xia, C. Wang, J. Li, P. Wu, L. Ma, Y. Wang, Y. Wang, F. Da, W. Liu, L. Xu, Enhancement of nitrite production via addition of hydroxylamine to partial denitrification (PD) biomass: Functional genes dynamics and enzymatic activities, Bioresource Technology, 318 (2020) 124274.
[24] F. Chen, X. Li, C. Gu, Y. Huang, Y. Yuan, Selectivity control of nitrite and nitrate with the reaction of S0 and achieved nitrite accumulation in the sulfur autotrophic denitrification process, Bioresource Technology, 266 (2018) 211-219.
[25] Y.-F. Deng, D. Wu, H. Huang, Y.-X. Cui, M.C.M. Van Loosdrecht, G.-H. Chen, Exploration and verification of the feasibility of sulfide-driven partial denitrification coupled with anammox for wastewater treatment, Water Research, 193 (2021) 116905.
[26] Y. Zhao, N.H. Ab Hamid, N. Reddy, M. Zheng, Z. Yuan, H. Duan, L. Ye, Wastewater Primary Treatment Using Forward Osmosis Introduces Inhibition to Achieve Stable Mainstream Partial Nitrification, Environmental Science & Technology, 56 (2022) 8663-8672.
[27] Z. Hu, T. Liu, Z. Wang, J. Meng, M. Zheng, Toward energy neutrality: novel wastewater treatment incorporating acidophilic ammonia oxidation, Environmental Science & Technology, 57 (2023) 4522-4532.
[28] Y. Wang, C. Bott, R. Nerenberg, Sulfur-based denitrification: Effect of biofilm development on denitrification fluxes, Water Research, 100 (2016) 184-193.
[29] Y. Wang, F. Sabba, C. Bott, R. Nerenberg, Using kinetics and modeling to predict denitrification fluxes in elemental-sulfur-based biofilms, Biotechnology and Bioengineering, 116 (2019) 2698-2709.
[30] S. An, K. Tang, M. Nemati, Simultaneous biodesulphurization and denitrification using an oil reservoir microbial culture: effects of sulphide loading rate and sulphide to nitrate loading ratio, Water research, 44 (2010) 1531-1541.
[31] M.-C. Simard, S. Masson, G. Mercier, H. Benmoussa, J.-F. Blais, L. Coudert, Autotrophic denitrification using elemental sulfur to remove nitrate from saline aquarium waters, Journal of Environmental Engineering, 141 (2015) 04015037.
[32] S. Agrawal, D. Seuntjens, P. De Cocker, S. Lackner, S.E. Vlaeminck, Success of mainstream partial nitritation/anammox demands integration of engineering, microbiome and modeling insights, Current opinion in biotechnology, 50 (2018) 214-221.
[33] M. Laureni, P. Falås, O. Robin, A. Wick, D.G. Weissbrodt, J.L. Nielsen, T.A. Ternes, E. Morgenroth, A. Joss, Mainstream partial nitritation and anammox: long-term process stability and effluent quality at low temperatures, Water Research, 101 (2016) 628-639.
[34] Y. Pan, B.-J. Ni, Z. Yuan, Modeling electron competition among nitrogen oxides reduction and N2O accumulation in denitrification, Environmental science & technology, 47 (2013) 11083-11091.
[35] M. Van Tendeloo, B. Bundervoet, N. Carlier, W. Van Beeck, H. Mollen, S. Lebeer, J. Colsen, S.E. Vlaeminck, Piloting carbon-lean nitrogen removal for energy-autonomous sewage treatment, Environmental Science: Water Research & Technology, 7 (2021) 2268-2281.

[36] A.A. Van De Graaf, P. De Bruijn, L.A. Robertson, M.S.M. Jetten, J.G. Kuenen, Autotrophic growth of anaerobic ammonium-oxidizing micro-organisms in a fluidized bed reactor, Microbiology, 142 (1996) 2187-2196.
[37] T. Bressani-Ribeiro, P.G.S. Almeida, C.A.L. Chernicharo, E.I.P. Volcke, Inorganic carbon limitation during nitrogen conversions in sponge-bed trickling filters for mainstream treatment of anaerobic effluent, Water Research, (2021) 117337.
[38] T.G. Vandekerckhove, K. Kobayashi, J. Janda, S. Van Nevel, S.E. Vlaeminck, Sulfur-based denitrification treating regeneration water from ion exchange at high performance and low cost, Bioresource technology, 257 (2018) 266-273.
[39] W. Lin, J. Feng, K. Hu, B. Qu, S. Song, K. He, C. Liu, Y. Chen, Y. Hu, Sulfidation forwarding high-strength Anammox process using nitrate as electron acceptor via thiosulfate-driven nitrate denitratation, Bioresource Technology, 344 (2022) 126335.
[40] M. Van Tendeloo, Y. Xie, W. Van Beeck, W. Zhu, S. Lebeer, S.E. Vlaeminck, Oxygen control and stressor treatments for complete and long-term suppression of nitrite-oxidizing bacteria in biofilm-based partial nitritation/anammox, Bioresource Technology, 342 (2021) 125996.
[41] A. APHA, Standard methods for the examination of water and wastewater analysis, American Public Health Association, Washington DC, (1998).
[42] H. Akoglu, User's guide to correlation coefficients, Turkish Journal of Emergency Medicine, 18 (2018) 91-93.
[43] Y. Xie, M. Spiller, S.E. Vlaeminck, A bioreactor and nutrient balancing approach for the conversion of solid organic fertilizers to liquid nitrate-rich fertilizers: Mineralization and nitrification performance complemented with economic aspects, Science of The Total Environment, 806 (2022) 150415.
[44] X. Zhang, P. Wu, L. Ma, J. Chen, C. Wang, W. Liu, L. Xu, A novel simultaneous partial nitrification and denitratation (SPND) process in single micro-aerobic sequencing batch reactor for stable nitrite accumulation under ambient temperature, Chemical Engineering Journal, 425 (2021) 130646.
[45] L.-D. Shi, T.-Y. Gao, X.-W. Wei, J.P. Shapleigh, H.-P. Zhao, pH-Dependent Hydrogenotrophic Denitratation Based on Self-Alkalization, Environmental Science & Technology, 57 (2023) 685-696.
[46] J. Almeida, M. Reis, M. Carrondo, Competition between nitrate and nitrite reduction in denitrification by Pseudomonas fluorescens, Biotechnology and Bioengineering, 46 (1995) 476-484.
[47] E.M. Meijer, J.W. Zwaan, A.H. Stouthamer, R. Wever, Anaerobic Respiration and Energy Conservation in Paracoccus denitrficans. Functioning of Iron-Sulfur Centers and the Uncoupling Effect of Nitrite, European Journal of Biochemistry, 96 (1979) 69-76.
[48] D.-J. Lee, X. Pan, A. Wang, K.-L. Ho, Facultative autotrophic denitrifiers in denitrifying sulfide removal granules, Bioresource Technology, 132 (2013) 356-360.
[49] C. Glass, J. Silverstein, Denitrification kinetics of high nitrate concentration water: pH effect on inhibition and nitrite accumulation, Water Research, 32 (1998) 831-839.
[50] J.L. Campos, S. Carvalho, R. Portela, A. Mosquera-Corral, R. Méndez, Kinetics of denitrification using sulphur compounds: Effects of S/N ratio, endogenous and exogenous compounds, Bioresource Technology, 99 (2008) 1293-1299.
[51] Y.-F. Deng, G.A. Ekama, Y.-X. Cui, C.-J. Tang, M.C.M. Van Loosdrecht, G.-H. Chen, D. Wu, Coupling of sulfur(thiosulfate)-driven denitratation and anammox process to treat nitrate and ammonium contained wastewater, Water Research, 163 (2019) 114854.
[52] T. Rohwerder, W. Sand, The sulfane sulfur of persulfides is the actual substrate of the sulfur-oxidizing enzymes from Acidithiobacillus and Acidiphilium spp, Microbiology, 149 (2003) 1699-1710.
[53] E.S. Boyd, G.K. Druschel, Involvement of intermediate sulfur species in biological reduction of elemental sulfur under acidic, hydrothermal conditions, Appl. Environ. Microbiol., 79 (2013) 2061-2068.
[54] E.S. Boyd, G.K. Druschel, Involvement of Intermediate Sulfur Species in Biological Reduction of Elemental Sulfur under Acidic, Hydrothermal Conditions, Applied and Environmental Microbiology, 79 (2013) 2061-2068.
[55] M.-F. Shao, T. Zhang, H.H.-P. Fang, Sulfur-driven autotrophic denitrification: diversity,

673 biochemistry, and engineering applications, Applied Microbiology and Biotechnology, 88
674 (2010) 1027-1042.
675 [56] A. Koenig, T. Zhang, L.-H. Liu, H.H.P. Fang, Microbial community and biochemistry
676 process in autosulfurotrophic denitrifying biofilm, Chemosphere, 58 (2005) 1041-1047.
677 [57] Q.-L. Wu, W.-Q. Guo, H.-S. Zheng, H.-C. Luo, X.-C. Feng, R.-L. Yin, N.-Q. Ren,
678 Enhancement of volatile fatty acid production by co-fermentation of food waste and excess
679 sludge without pH control: The mechanism and microbial community analyses, Bioresource
680 Technology, 216 (2016) 653-660.
681 [58] L. Zhang, C. Zhang, C. Hu, H. Liu, Y. Bai, J. Qu, Sulfur-based mixotrophic denitrification
682 corresponding to different electron donors and microbial profiling in anoxic fluidized-bed
683 membrane bioreactors, Water Research, 85 (2015) 422-431.
684 [59] R. Du, S. Cao, S. Wang, M. Niu, Y. Peng, Performance of partial denitrification (PD)-
685 ANAMMOX process in simultaneously treating nitrate and low C/N domestic wastewater at
686 low temperature, Bioresource Technology, 219 (2016) 420-429.
687 [60] S. Cao, B. Li, R. Du, N. Ren, Y. Peng, Nitrite production in a partial denitrifying upflow
688 sludge bed (USB) reactor equipped with gas automatic circulation (GAC), Water Research, 90
689 (2016) 309-316.
690 [61] S. Agrawal, D. Seuntjens, P.D. Cocker, S. Lackner, S.E. Vlaeminck, Success of
691 mainstream partial nitritation/anammox demands integration of engineering, microbiome and
692 modeling insights, Current Opinion in Biotechnology, 50 (2018) 214-221.
693 [62] M. Strous, J.J. Heijnen, J.G. Kuenen, M.S.M. Jetten, The sequencing batch reactor as a
694 powerful tool for the study of slowly growing anaerobic ammonium-oxidizing microorganisms,
695 Applied Microbiology and Biotechnology, 50 (1998) 589-596.
696 [63] M. Tomaszewski, G. Cema, A. Ziembińska-Buczyńska, Influence of temperature and pH
697 on the anammox process: A review and meta-analysis, Chemosphere, 182 (2017) 203-214.
698 [64] F. Xie, B. Zhao, Y. Cui, X. Ma, D. Li, X. Yue, Enhancing nitrogen removal performance
699 of anammox process after short-term pH and temperature shocks by coupling with iron-carbon
700 micro-electrolysis, Journal of Cleaner Production, 289 (2021) 125753.

701

Table 1. Correlation analysis of (a) the residual NO_3^--N, and NAE during different operational phases; (b) BSNLR with NAE, BSNAR, NRE, and residual NO_3^--N. The p-values and Spearman's ρ are reported.

(a)

Phase	I-VII	I	II	III	IV	V	VI	VII
p-value	**< 0.0001**	0.31	0.38	0.20	**0.05**	0.07	**< 0.0001**	**0.02**
ρ	0.48	0.41	0.34	0.44	0.39	0.77	0.87	0.47

(b)

	NAE	BSNAR	NRE	Residual NO_3^--N
p-value	**< 0.0001**	**< 0.0001**	**< 0.0001**	**< 0.0001**
ρ	0.61	0.78	0.7	0.75

Figure Captions

Figure 1. NH_4^+-N concentration in influent ("in"), effluent ("ef"), and the ratio of NH_4^+-N loss to influent NH_4^+-N concentration during the experiment.

Figure 2. (a) NO_3^--N concentration in the influent ("in") and effluent ("ef"), and the accumulated NO_2^--N in the effluent ("ef"); (b) NO_3^--N removal efficiency (NRE) and NO_2^--N accumulation efficiency (NAE) under pH control condition; (c) NO_3^--N loading rate (NLR) and conversion rate, NO_2^--N accumulation rate, and biomass-specific nitrate loading rate (BSNLR) from day 0 to day 130. The blue shadings in phases II, IV, and VI mean pH control at around 8.5.

Figure 3. The ratio of accumulated NO_2^--N to NH_4^+-N in the effluent, and the ideal ratio (i.e., 1.3) for anammox. The blue shadings in phases II, IV, and VI mean pH control at around 8.5.

Figure 4. The relative abundance of the sulfurotrophic community at genus levels during the reactor operation. BC dissimilarity represents the Bray-Curtis dissimilarity between the first and each subsequent sample.

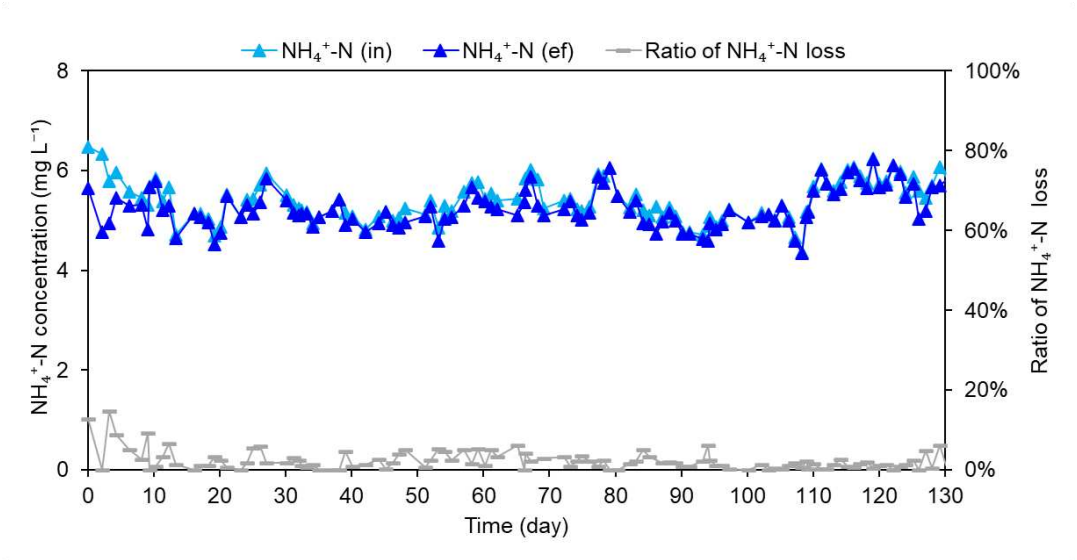

Figure 1. NH_4^+-N concentration in influent ("in"), effluent ("ef"), and the ratio of NH_4^+-N loss to influent NH_4^+-N concentration during the experiment.

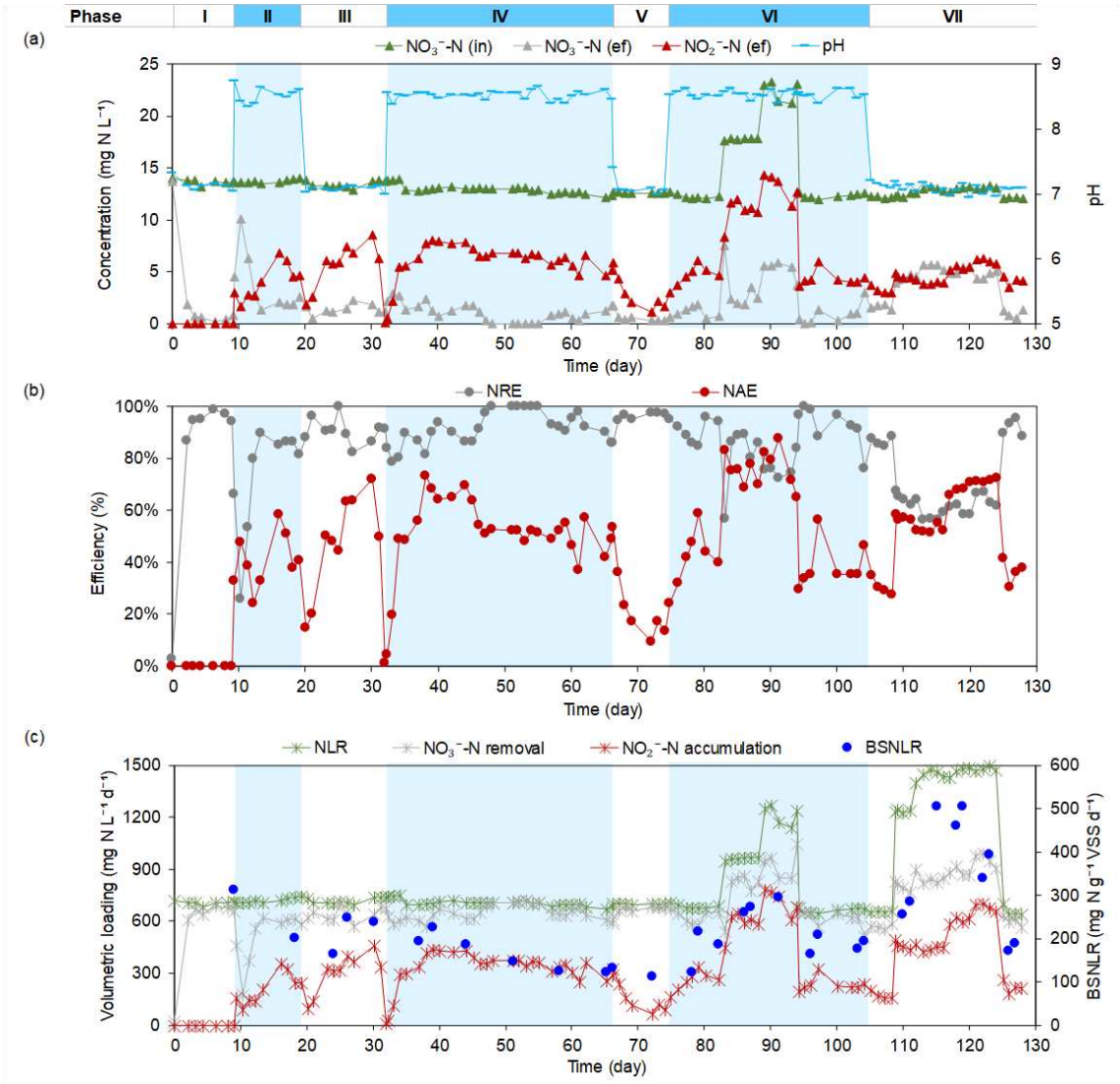

Figure 2. (a) NO_3^--N concentration in the influent ("in") and effluent ("ef"), and the accumulated NO_2^--N in the effluent ("ef"); (b) NO_3^--N removal efficiency (NRE) and NO_2^--N accumulation efficiency (NAE) under pH control condition; (c) NO_3^--N loading rate (NLR) and conversion rate, NO_2^--N accumulation rate, and biomass-specific nitrate loading rate (BSNLR) from day 0 to day 130. The blue shadings in phases II, IV, and VI mean pH control at around 8.5.

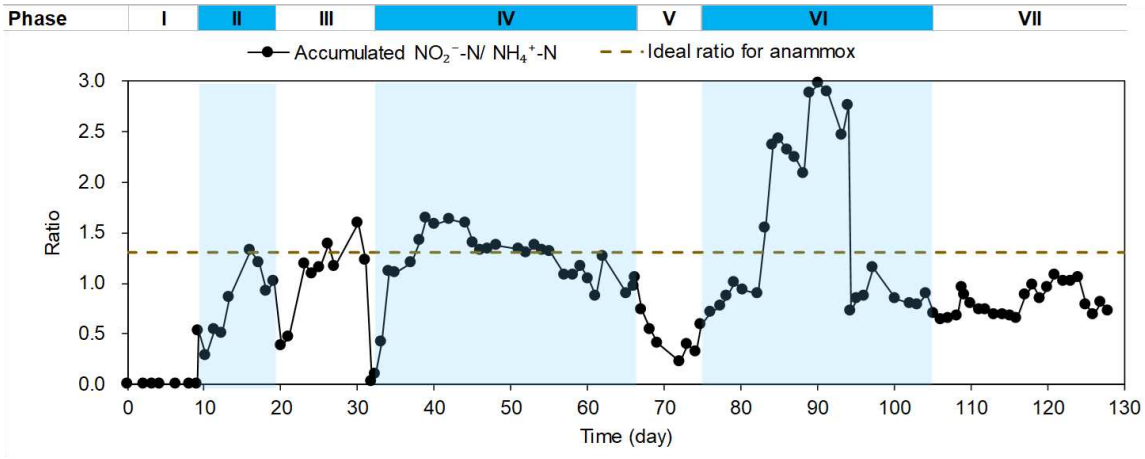

Figure 3. The ratio of accumulated NO_2^--N to NH_4^+-N in the effluent, and the ideal ratio (i.e., 1.3) for anammox. The blue shadings in phases II, IV, and VI mean pH control at around 8.5.

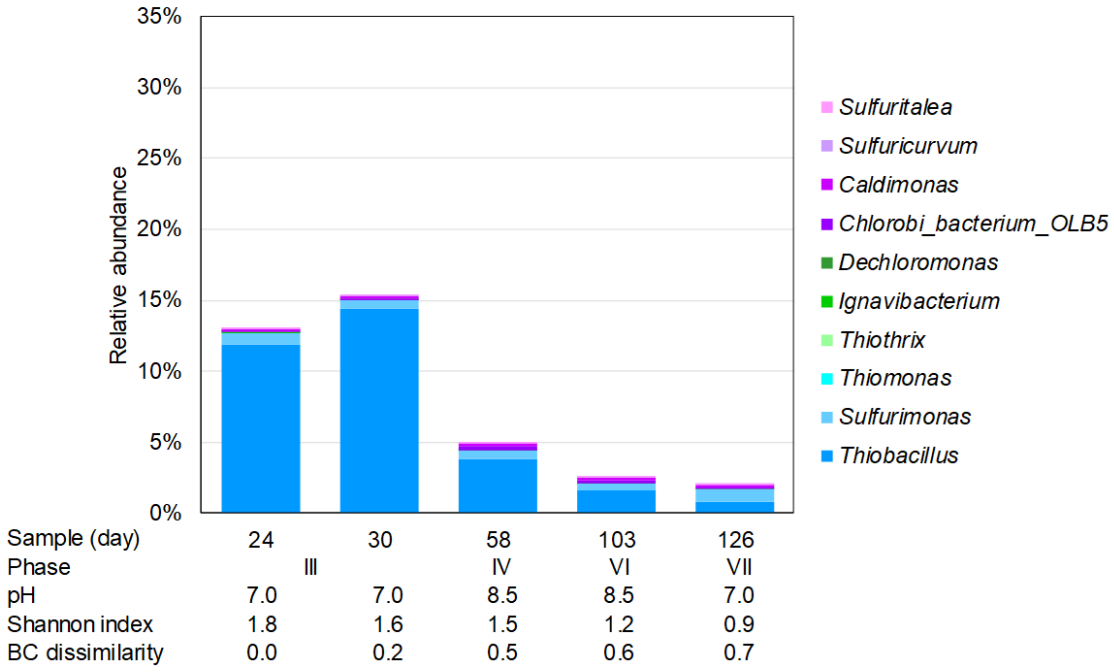

Figure 4. The relative abundance of the sulfurotrophic community at genus levels during the reactor operation. BC dissimilarity represents the Bray-Curtis dissimilarity between the first and each subsequent sample.